

# High-Linearity and Temperature-Insensitive 2.4 GHz SiGe Power Amplifier with Dynamic-Bias Control

Wei-Chun Hua<sup>1</sup>, Hung-Hui Lai<sup>1</sup>, Po-Tsung Lin<sup>1</sup>, Chee Wee Liu<sup>1,\*</sup>, Tzu-Yi Yang<sup>2</sup>, and Gin-Kou Ma<sup>2</sup>

<sup>1</sup>Department of Electrical Engineering and Graduate Institute of Electronics Engineering, National Taiwan University, Taiwan, R. O. C. \*chee@cc.ee.ntu.edu.tw

<sup>2</sup>SoC Technology Center, Industrial Technology Research Institute, Taiwan, R.O.C.

**Abstract** — A high-linearity and temperature-insensitive 2.4 GHz power amplifier (PA) with dynamic-bias control is realized in a SiGe HBT technology with 0.9  $\mu\text{m}$  emitter width. Due to the bias linearization, the  $P_{1\text{dB}}$  of 27 dBm is only 0.5 dB smaller than  $P_{\text{sat}}$ , which is the record low to the best of our knowledge. With simple temperature-insensitive bias, the total current deviations from the room temperature are smaller than 6% and 10% at the linear  $P_{\text{out}}$  (24/20 dBm) for 802.11b and 802.11g, respectively at the test temperature from 0 °C to 85 °C. The integrated power detector has a wide dynamic range of 20 dB. The DC current can be reduced to 53 mA and the power-added-efficiency (PAE) can be enhanced up to 3 times at low  $P_{\text{out}}$  level under dynamic-bias control operation, and meanwhile the 802.11b/g linearity requirements are achieved. This design is most suitable for the future 802.11n application due to its high linearity.

**Index Terms** — Dynamic-bias control, linearization, power amplifier, temperature-insensitive, and WLAN.

## I. INTRODUCTION

There are several WLAN (Wireless Local Area Network) standards operated at 2.4 GHz band, such as IEEE 802.11b/g and the developing high-throughput standard (802.11n, >100 Mbps). To have higher throughput in the same bandwidth, spectrum-efficient modulation, such as OFDM, is adopted for 802.11g/n wireless data transmission. Since the OFDM signal has

very high peak to average ratio, the resulting strict linearity requirements on spectral regrowth and error vector magnitude (EVM) make the CMOS PA hard to achieve. In order to lower the cost and to improve the power characteristics, SiGe HBT technology becomes the best candidate for the high-throughput WLAN PA.

There are several techniques to enhance the linearity of the PA, such as predistortion [1], variable feedback [2], and active bias linearization [3]. Among those methods, the active bias linearization shows the greatest enhancement. Therefore, the basic concept of the active bias linearization is adopted in this paper and its performance is further enhanced by adding the temperature-insensitive function to operate stably over wide temperature range. The DC power consumption and PAE at low output power level can be improved under dynamic-bias control operation [4].

## II. DEVICE TECHNOLOGY

The emitter width and length of the unit cell are 0.9  $\mu\text{m}$  and 20.3  $\mu\text{m}$ , respectively and there are four fingers in a unit cell. In order to ensure the high-power operation, the high-voltage type device is used with a  $BV_{\text{ceo}}$  of 6 V. The measured  $f_T$  and  $f_{\text{max}}$  of the unit cell are 25 GHz and 32 GHz, respectively.

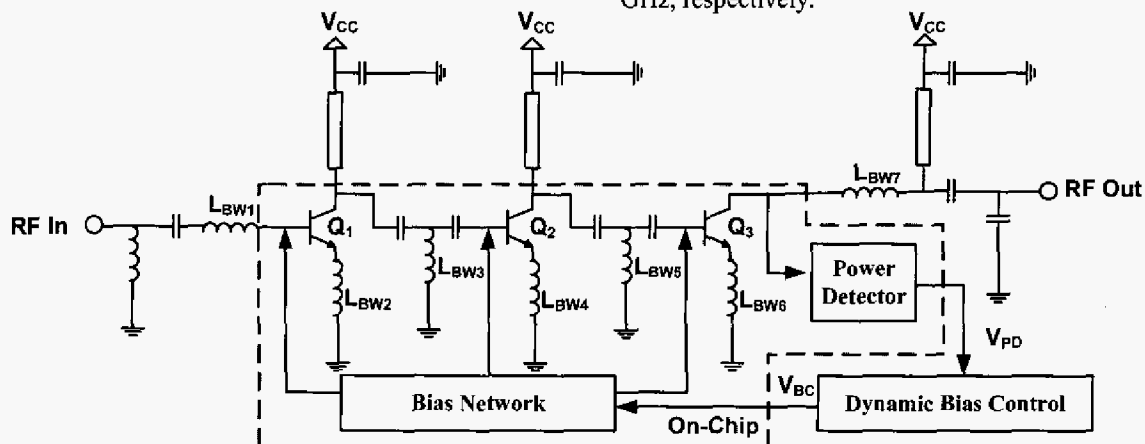


Fig. 1 Simplified circuit diagram of the power amplifier.

### III. CIRCUIT DESIGN

Fig. 1 shows the simplified circuit diagram of the PA. The PA consists of three single-ended common-emitter stages with integrated active bias linearizer and power detector (PD). The inter-stage matching networks are designed partially on-chip while the I/O matching networks are accomplished off-chip to optimize the PA performances. The inductors with the suffixes of "BW" are the bond wire inductors. To overcome the low Q on-chip inductor, the high-pass T-matching topology is adopted in the inter-stage matching. The shunt inductors in the inter-stage matching networks can be fulfilled using bond wire inductors and the resulting PA chip is inductorless. The low-pass output matching network is used to filter out the harmonics.

The collector DC voltages ( $V_{CC}$ ) of each stage are fed through quarter-wavelength transmission lines on the FR4 PCB which function as the RF chokes. Various values of the bypass capacitors are placed between the  $V_{CC}$  node and the ground to filter out wide frequency range of noises.

#### A. Bias Network

Fig. 2 shows the bias network of the PA. The transistors,  $Q_2$  and  $Q_4$ , act as the current mirror which provides the base bias current of the core transistor ( $Q_1$ ). The bias current is controlled by the bias control voltage ( $V_{BC}$ ) and  $R_1$ . Since the DC voltage of the base node of  $Q_4$  is about twice of the base-emitter junction voltage, a diode-connected transistor ( $Q_3$ ) is added to the left branch of the bias circuit to maintain the proper DC level. The linearization mechanism is achieved by the base-emitter junction diode of  $Q_4$  and the bypass capacitor  $C_1$  [3]. The bias linearizer can provide the increase of the base voltage and the collector current of  $Q_1$  as the input power increases. Thus the class-A operating range can be extended to higher input power level to postpone the occurrence of the current waveform clipping and results in higher output  $P_{out}$ .

The temperature-insensitive function can be achieved by adding resistors in the bias current path, such as  $R_1$ ,  $R_2$ , and  $R_3$  in Fig. 2. The design equation to minimize the base-emitter voltage mismatch between  $Q_2$  and  $Q_4$  over temperature variation is listed below:

$$\frac{A_E(Q_4)}{A_E(Q_2)} = \frac{R_2}{(\beta_4 - 1)R_3} \quad (1)$$

where  $A_E(Q_2)$ ,  $A_E(Q_4)$ , and  $\beta_4$  are the emitter area of  $Q_2$ ,  $Q_4$ , and the current gain of  $Q_4$ , respectively. The resistors in the bias network can reduce (increase) the base-emitter voltages of  $Q_2$  and  $Q_4$  when the bias current

increases (decreases). As a result, the bias current can be stabilized over wide temperature variation. Since  $R_3$  causes additional power loss and raises the input impedance of the bias network to degrade the linearization mechanism, a bypass capacitor ( $C_2$ ) is added parallel to  $R_3$  to maintain the linearization and temperature-insensitive functions simultaneously.

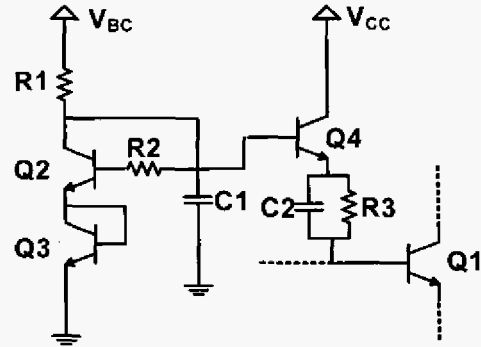


Fig. 2 Linearization and temperature-insensitive bias circuit.

#### B. Integrated Power Detector Circuit

Fig. 3 shows the integrated power detector circuit of the PA. The transistor  $Q_1$  represents the PA transistor of the 3<sup>rd</sup>-stage. The PD sense the output power level through the collector node of  $Q_1$ , the input impedance of the PD should be very high to prevent the power leakage to the PD. The base-emitter-shorted transistor ( $Q_2$ ) is the major part of the PD. The base-collector junction is used since it is more robust than the base-emitter junction due to its lower doping level and thus higher breakdown voltage. When an increasing sinusoidal voltage presents at the output node (collector of  $Q_1$ ), the base current of  $Q_2$  has an increasing DC level due to the exponential current-voltage relation of a diode ( $I_C - V_{BC}$ ). The DC current flows from  $V_{CC}$ , and then flows through  $R_1$ ,  $Q_2$  and,  $R_L$  to

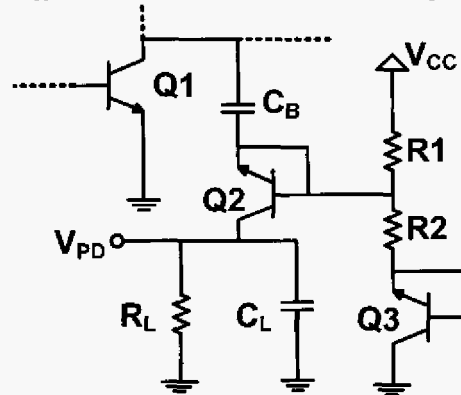


Fig. 3 Integrated power detector with temperature compensation

generate the power detector voltage ( $V_{PD}$ ). The minimal DC level of the  $V_{PD}$  can be tailored by the quiescent point of  $Q_2$  through the resistive voltage-divider and  $Q_3$ . With the base-emitter-shorter transistor ( $Q_3$ ) at the resistive bias branch, the PD circuit can be less sensitive to the temperature variation.

#### IV. MEASUREMENT RESULTS

Fig. 4 shows the die photo of the PA. The emitter-grounding inductance is crucial for the single-ended RF PA. Since the Si-based technology has no low-parasitic via-hole process, special treatments such as flip-chip [5] or heavily-doped sinker [6] are used in the literatures. In this paper, double-bond-wires (at a single pad) are used to minimize the emitter inductive-degeneration effect. Fig. 5 shows the power characteristics of the PA at 2.45 GHz. The small signal gain,  $P_{sat}$ , and  $P_{1dB}$  are 22.2 dB, 27.5 dBm, and 27 dBm, respectively. The effect of the linearization bias is clearly observed from the gain expansion phenomenon. The maximum linear  $P_{out}$  that meets the spectrum mask requirements of the 802.11b standard (11 Mbps, CCK signal) at 2.45 GHz is 24dBm.

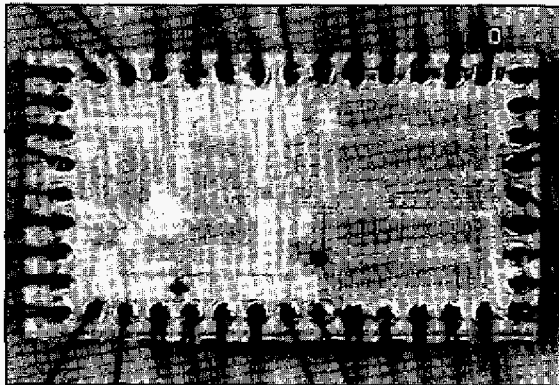


Fig. 4 The die photo of the PA (1.48 mm x 0.88 mm).

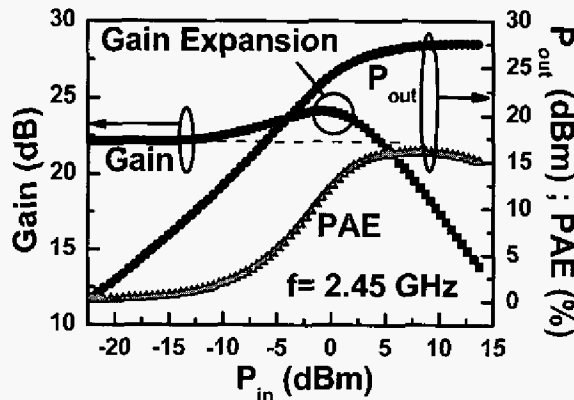


Fig. 5 The power characteristics of the PA at 2.45 GHz. The small signal gain is 22.2 dB, the  $P_{sat}$  is 27.5 dBm, and the  $P_{1dB}$  is 27 dBm.

The maximum linear  $P_{out}$  with EVM of 3.5%, which has better spectrum mask and EVM than the 802.11g standard (54 Mbps OFDM signal, 64QAM) is 20dBm. The PAEs at the linear  $P_{out}$  of 24 dBm (11b) and 20 dBm (11g) are 12.2% and 7.2%, respectively.

Fig. 6 shows the total current versus power for 0, 25, and 85 °C. The total current variations ( $\Delta I_{CC}$ ) compared to the total current at 25°C are smaller than 6% and 10% at the linear  $P_{out}$  for 802.11b, and g, respectively. The resulting  $\Delta I_{CC}$  is comparable with the commercial 802.11b/g SiGe PA product (e.g. SE2529L of SiGe semiconductor Inc.,  $|\Delta I_{CC}| < 10\%$  from -40°C to 85°C).

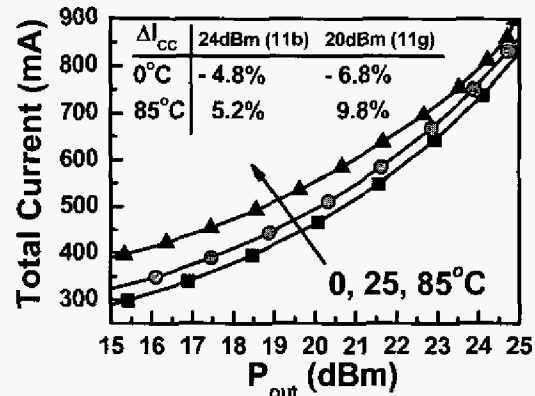


Fig. 6 The total current of the PA versus output power for different temperatures. The  $\Delta I_{CC}$  comparisons are based on the data measured at 25°C.

Fig. 7 shows the diagram of  $V_{PD}$  versus  $P_{out}$  for different temperatures. The variation of the  $V_{PD}$  (0 °C to 85 °C) is smaller than 0.1 V. The dynamic range of the PD is ~20 dB (5-25 dBm).

Fig. 8 shows the gain and the DC bias current versus bias control voltage ( $V_{bc}$ ). The tuning range of the  $V_{bc}$  is 1 V with the gain slope of ~13.5 dB/V. The DC bias current can be as low as 53 mA when  $V_{bc}$  is set to 1.4 V.

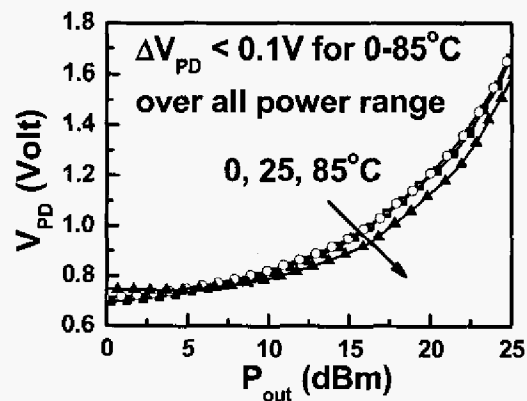


Fig. 7 The power detector voltage ( $V_{PD}$ ) versus output power for different temperatures.

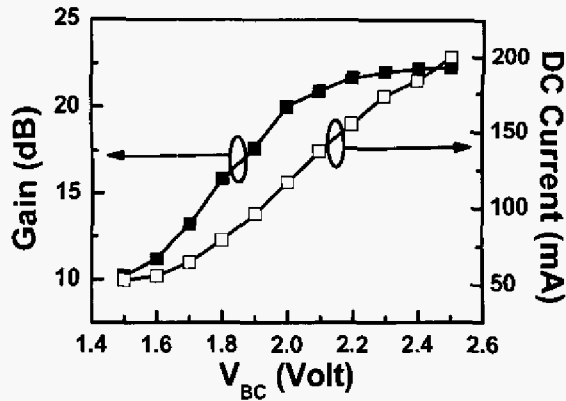


Fig. 8 The gain and the DC bias current versus the bias control voltage.

Fig. 9 shows the PAE and the EVM versus  $P_{out}$  under fixed-bias and dynamic-bias operations. At low  $P_{out}$ , the DC current is reduced, and meanwhile the linearity requirements of 802.11b/g standards are achieved. When the needed  $P_{out}$  is lower than 20 dBm, the bias current is adjusted to the minimum value that satisfies the spectrum mask and the EVM ( $< 3.5\%$ ) requirements of 802.11g. Since the PA related linearity requirements of the 802.11b standard is looser than those of the 802.11g standard, the resulting PA can also work for the 802.11b application. The PAE at 8 dBm  $P_{out}$  can be enhanced up to 3 times under dynamic-bias operation. Once the optimum bias for each  $P_{out}$  is determined, the control mechanism can be realized in the baseband chip to give proper  $V_{BC}$  according to the desired  $P_{out}$ . The PA performances are summarized in table I.

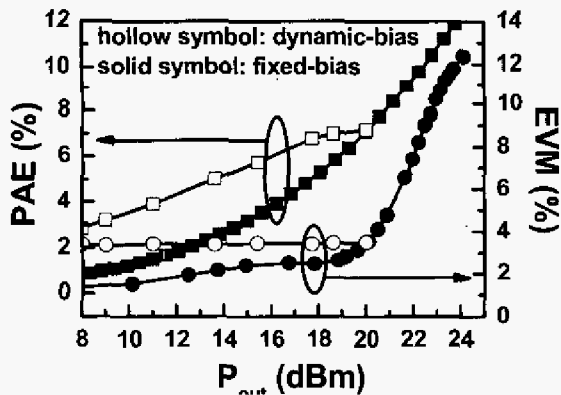


Fig. 9 The PAE and EVM performances versus  $P_{out}$  for dynamic-bias and fixed-bias operations.

## V. CONCLUSIONS

A high-linearity and temperature-insensitive SiGe PA for 802.11b/g WLAN applications is demonstrated in this paper, and which is also promising for the future high-throughput 802.11n application due to its high linearity. The simple temperature-insensitive bias can provide

comparable temperature stability as the commercial SiGe PA product. The dynamic-bias control mechanism can dramatically reduce the bias current and enhance the PAE at low  $P_{out}$  level to achieve low DC power consumption and high linear  $P_{out}$  simultaneously.

TABLE I  
PERFORMANCE SUMMARY

Frequency (GHz)	2.45
Supply Voltage (V)	3.3
DC Bias Current (mA)	180 ; 53*
Gain (dB)	22.2
$P_{sat}$ (dBm)	27.5
$P_{1dB}$ (dBm)	27
Linear $P_{out}$ (dBm)	20 (11g) ; 24 (11b)
PAE @ linear $P_{out}$ (%)	7.2 (11g) ; 12.2 (11b)
Current Deviation from Room Temperature (%) (0-85 °C)	$< 6\%$ (24 dBm) $< 10\%$ (20dBm)
EVM @ 20 dBm (%)	3.5%
Power Detector Dynamic Range (dBm)	5-25
$V_{PD}$ Variation (V) for 0-85 °C	$< 0.1$
Gain Slop of $V_{BC}$ (dB/V)	13.5

\*Dynamic-bias operation

## REFERENCES

- [1] N. Gupta, A. Tombak, and A. Mortazawa, "A Varactor Diode Based Predistortion Circuit," *2004 IEEE MTT-S Int. Microwave Symp. Dig.*, vol. 2, pp. 689-692, June 2004.
- [2] K. Fujita, K. Shirakawa, N. Takahashi, Y. Liu, T. Oka, M. Yamashita, K. Sakuno, H. Kawamura, M. Hasegawa, H. Koh, K. Kagoshima, H. Kijima, and H. Sato, "A 5GHz High Efficiency and Low Distortion InGaP/GaAs HBT Power Amplifier MMIC," *2003 IEEE MTT-S Int. Microwave Symp. Dig.*, vol. 2, pp. 871-874, June 2003.
- [3] Y. S. Noh and C. S. Park, "PCS/W-CDMA Dual-Band MMIC Power Amplifier with a Newly Proposed Linearization Bias Circuit," *IEEE J. Solid-State Circuits*, vol. 37, no.9, pp. 1096-1099, Sept. 2002.
- [4] Y. -W. Kim, K. -C. Han, S.-Y. Hong, and J. -H. Shin, "A 45% PAE/18mA Quiescent Current CDMA PAM with a Dynamic Bias Control Circuit," *2004 IEEE Radio Frequency Integrated Circuits Symp. Dig.*, pp. 365-368.
- [5] W. Bischof, M. Alles, S. Gerlach, A. Kruck, A. Schüppen, J. Sinderhauf, and H. -J. Wassener, "SiGe-Power Amplifiers in Flipchip and Packaged Technology," *2001 IEEE Radio Frequency Integrated Circuits Symp. Dig.*, pp. 35-38.
- [6] W. Bakalski, K. Kitlinski, G. Doing, B. Kapfelsperger, W. Österreicher, W. Aughter, R. Weigel, and A. L. Scholtz, "A 5.25 GHz SiGe Bipolar Power Amplifier for IEEE 802.11a Wireless LAN," *2004 IEEE Radio Frequency Integrated Circuits Symp. Dig.*, pp. 567-570.